Thermal and radiation-enhanced diffusion in the bulk metallic glass $Ni_{23}Zr_{62}Al_{15}$

S. Flege and H. Hahn
Institute of Materials Science, Darmstadt University of Technology, Petersenstr. 23, 64287 Darmstadt, Germany

R. S. Averback
Department of Materials Science and Engineering, University of Illinois at Urbana-Champaign, Urbana, Illinois, USA

(Received 21 May 2003; revised manuscript received 25 September 2003; published 29 January 2004)

The temperature dependence of tracer diffusion in the three-component system NiZrAl was measured. For the composition $Ni_{23}Zr_{62}Al_{15}$, it was possible to measure diffusion coefficients below and above the glass transition temperature. Similar to the binary metallic glass NiZr, the diffusion coefficient was strongly dependent on the atomic size of the tracer, varying by two orders of magnitude. The results are suggestive of a collective diffusion mechanism in bulk metallic glasses. Radiation-enhanced diffusion was also measured in this alloy and compared with measurements of radiation-induced viscous flow on similar alloys.

DOI: 10.1103/PhysRevB.69.014303 PACS number(s): 66.30.Jt, 61.43.Dq

I. INTRODUCTION

A strong dependence of diffusion coefficients on the atomic size of the tracer atoms has been observed in many binary amorphous alloy systems. This effect was first noted in the alloy Ni_xZr_{100-x},[1] and led to the conclusion that two distinct diffusion mechanisms were possible: an interstitial-like process for smaller atoms and a collective one for larger atoms. The packing density of a binary metallic glass is reported to increase by alloying with Al.[2] Al has an intermediate atomic size, compared with Ni and Zr, and thus can fill the free volume within the disordered structure of the glass. The increased packing results in a reduced atomic mobility of the alloy components, which possibly explains the existence of a significant supercooled liquid region in these alloys. The difference between the glass transition temperature and the crystallization temperature is ≈ 75 K for the example of $Ni_{25}Zr_{60}Al_{15}$. (Strictly speaking this value is only true for a heating rate of 0.67 K/s (40 K/min) since the glass transition is time and temperature dependent, cf. e.g., Ref. 3. In the following, however, this value will be taken as a reference, because the small mass of sample material in our case did not permit measurements with a differential scanning calorimeter.) In contrast the glass transition in the absence of Al, i.e. in NiZr, is too small to readily observe.[4]

Although the reduction of the diffusion coefficients in $Ni_{25}Zr_{60}Al_{15}$ has been postulated and surmised from its solidification characteristics,[5] it has not been measured directly in a systematic manner. We have demonstrated recently, however, that there is a decrease of the diffusion coefficients with additions of Al to NiZr.[6] In the ternary system NiZrAl, the compositions in the region $Ni_{25}Zr_{60}Al_{15}$ are of particular interest since supercooled liquids of these alloys exist over a large range of temperatures. In this paper, we concentrate on an alloy with composition $Ni_{23}Zr_{62}Al_{15}$, which is in the middle of the composition field of alloys having large undercooling.

The amount of free volume is increased significantly as the glass transition temperature T_g is reached. Concurrent with this change of the structure of the amorphous matrix is an increased atomic mobility, which is reflected in an increased slope of the Arrhenius plot. This effect has been observed in several bulk metallic glasses, e.g., ZrTiCuNiBe.[7,8] The atomic transport mechanism, however, is believed to be still solidlike thermally activated hopping.[9] In contrast to these experiments, which have investigated mainly the self-diffusion, we performed diffusion studies with tracer impurities (Co, Fe, Cu, Ti, and Hf), which are similar in atomic size to the matrix components Ni, Zr, and Al; cf. Table I.

Only a few measurements of radiation-enhanced diffusion (RED) on amorphous metals have been reported. They are useful, however, since if point defects were vehicles for diffusion, radiation-induced vacancies would reduce the effective activation enthalpy Q. On the other hand, if the diffusion occurs by a collaborative motion of several atoms, there should be no influence on the activation enthalpy. Both tendencies have been observed, a reduction of Q in NiZr (Ref. 10) and FeNiB,[11] and no influence in CoNiFeSiB.[12] The effect observed is likely to depend on the mass of the projectile.[13] Our investigation is limited to the high-energy-transferred irradiation, because only results of this kind are available for NiZr. For the effect of low-energy-transferred irradiation cf. Ref. 14.

For the present diffusion experiments, we have selected a thin film geometry containing an embedded layer of tracer

TABLE I. Atomic size of the components of the alloy and the tracers used.

Element	Size (nm)
Ni	0.124
Co	0.125
Fe	0.127
Cu	0.128
Al	0.143
Ti	0.147
Hf	0.158
Zr	0.160

atoms. This sample geometry enables easy depth profiling, ideal incorporation of the tracer layer and ease in altering the composition of the alloy during growth.

II. EXPERIMENTAL TECHNIQUES

The thin film samples were prepared in an ultra high vacuum molecular deposition system (MBE) with four electron beam evaporators, one for the tracer metal and three rate controlled evaporators for the matrix components (Ni, Zr, Al). Oxidized Si-wafers (3-in. diameter) maintained near room temperature were used as substrates. The tracer layers were deposited without interrupting the growth of the metallic glass, thus avoiding discrete interfaces. The film, which was $\approx 200-300$ nm thick, contained the t racer layer at a depth of ≈ 100 nm from the substrate. The tracer atoms were initially spread over a region ≈ 3 nm thick, using a shuttering system. The tracer concentration in this region was initially $\approx 20\%$.

Prior to the diffusion anneals the samples were cut into small pieces. For the temperature range between 473 and 703 K, annealing was performed under high vacuum conditions ($p < 10^{-5}$ Pa) with a resistance wire heated furnace. For the higher temperatures, up to 763 K, and corresponding shorter annealing times, a rapid thermal processing unit with ultraviolet-light heating was employed with a heating rate of 15 K/s. Annealing in the latter case was performed in an Ar atmosphere. The accuracy of the temperature measurement was ± 2 K at the higher temperatures and ± 1 K at the lower temperatures. Several cross-checks, such as annealing at the same temperature in both annealing facilities, were performed to rule out experimental artifacts.

The irradiations were performed with Kr^+ ions with energies of 1 and 2 MeV for Hf and Co tracers, respectively. The beam was scanned to provide a homogeneous flux; an aperture, 3 mm in diameter, defined the area of the beam. The total ion dose for all irradiations was 1×10^{16} cm^{-2}, while ion current was limited to ≈ 100 nA to reduce beam heating.

The amorphous structure of the films, both before and after all diffusion anneals, was checked using x-ray diffraction. The composition of the samples was determined with Rutherford backscattering spectroscopy using 2- or 3-MeV He^+ and a backscattering angle of 171°. The concentration-depth profiles of the tracer atoms were determined using secondary ion mass spectrometry (SIMS) with 8-keV O_2^+ primary ions (Cameca ims 5f). Assuming a Gaussian distribution for the tracer profile before and after annealing, the diffusion coefficient D was obtained using the expression,

$$Dt = \tfrac{1}{2}(\sigma^2_{annealed} - \sigma^2_{unannealed}), \qquad (1)$$

where t is the annealing time. The sputter erosion rate in the SIMS was obtained by measuring the depth of the sputter crater using a Dektak IIa profilometer.

III. RESULTS

A. Thermal diffusion

Representative examples of concentration-depth profiles as obtained by SIMS can be found in Fig. 1, the thermal

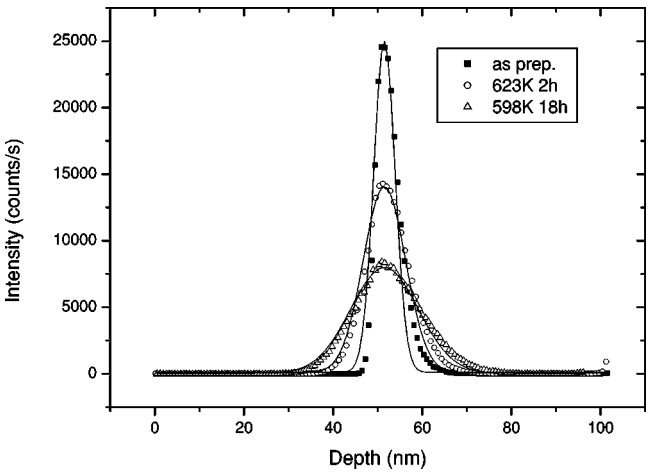

FIG. 1. Concentration-depth profile of ^{56}Fe in $Ni_{23}Zr_{62}Al_{15}$ before (as prep.) and after annealing (623 K 2 h and 598 K 18 h) obtained by SIMS. The symbols represent the measured values, the lines are the fits to the data.

diffusion coefficients of all tracers (Co, Fe, Cu, Ti, Hf) in the temperature range 508–763 K are summarized in Fig. 2 and Table II. The temperature range is smaller for Ti and Hf due to their smaller diffusion coefficients. The experimental errors in the absolute diffusivities are largest, $\approx 20\%$, for samples with the smallest diffusivities, $\approx 5\times10^{-24}$ m^2 s^{-1}. All curves exhibit an Arrhenius behavior both above and below T_g. Above T_g, i.e., ≈ 700 K, however, the slopes in the Arrhenius curves are larger for the tracers Co, Ti, and Hf. The values of the activation enthalpy, Q, (accuracy ± 0.15 eV) and the pre-exponential factor, D_0, are given in Tables III and IV for the temperature range below T_g and above T_g, respectively. For comparison, the data for Co and Hf diffusion in $Ni_{50}Zr_{50}$, calculated from the values for Q and D_0 provided in Refs. 15 and 16, respectively, are indicated by the dotted lines in Fig. 2.

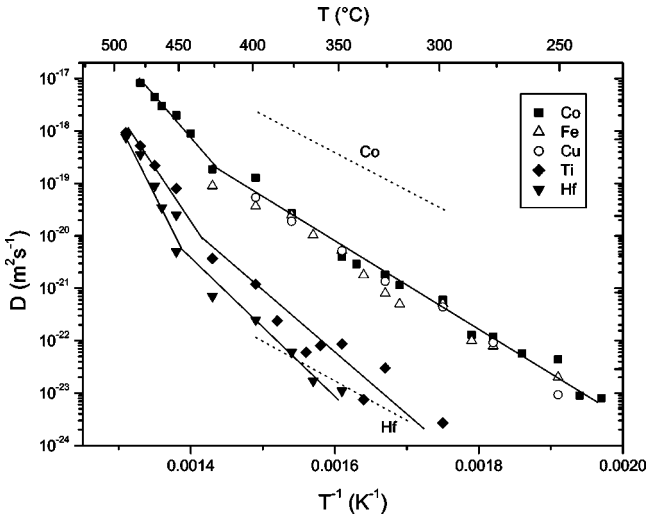

FIG. 2. Diffusion coefficients D of various tracers in $Ni_{23}Zr_{62}Al_{15}$. The dotted lines indicate the diffusion of Co (Ref. 15) and Hf (Ref. 16) in $Ni_{50}Zr_{50}$.

TABLE II. Annealing temperature and time and diffusivity for the tracer elements Co, Fe, Cu, Ti, and Hf.

Tracer	Temperature (K)	Annealing time (s)	Diffusivity ($m^2\,s^{-1}$)	Tracer	Temperature (K)	Annealing time (s)	Diffusivity ($m^2\,s^{-1}$)
Co	508	230400	8.0×10^{-24}	Cu	523	172800	9.3×10^{-24}
	516	518400	9.0×10^{-24}		548	64800	9.2×10^{-23}
	523	86400	4.4×10^{-23}		573	18000	4.4×10^{-20}
	538	86400	5.7×10^{-23}		598	18000	1.4×10^{-21}
	548	64800	1.2×10^{-22}		623	7200	5.2×10^{-21}
	560	64800	1.3×10^{-22}		648	3600	1.9×10^{-20}
	573	18000	6.0×10^{-22}		673	1800	5.4×10^{-20}
	593	7200	1.2×10^{-21}	Ti	573	248400	2.7×10^{-24}
	598	4500	1.8×10^{-21}		598	259200	3.0×10^{-23}
	613	2700	2.9×10^{-21}		608	252000	7.5×10^{-24}
	623	5400	4.0×10^{-21}		623	43200	8.7×10^{-23}
	643	2400	2.7×10^{-20}		633	64800	8.0×10^{-23}
	673	1200	1.3×10^{-19}		643	32400	6.0×10^{-23}
	698	1200	1.9×10^{-19}		658	28800	2.4×10^{-22}
	713	120	9.0×10^{-19}		673	2700	1.2×10^{-21}
	723	450	2.0×10^{-18}		698	1800	3.7×10^{-21}
	733	330	3.0×10^{-18}		723	600	8.0×10^{-20}
	743	60	4.5×10^{-18}		743	240	2.2×10^{-19}
	753	60	8.2×10^{-18}		753	120	5.2×10^{-19}
Fe	523	230400	2.0×10^{-23}		763	60	9.3×10^{-19}
	548	18000	7.9×10^{-23}	Hf	623	180000	1.1×10^{-23}
	560	72000	1.0×10^{-22}		638	259200	1.7×10^{-23}
	573	5400	5.1×10^{-22}		648	158400	6.0×10^{-23}
	593	10800	5.0×10^{-22}		673	18000	2.5×10^{-22}
	598	14400	8.0×10^{-22}		698	36000	7.0×10^{-22}
	611	14400	1.8×10^{-21}		721	18000	5.0×10^{-21}
	623	7200	5.3×10^{-21}		723	600	2.5×10^{-20}
	635	1800	1.0×10^{-20}		733	600	3.5×10^{-20}
	648	2400	2.5×10^{-20}		743	240	9.0×10^{-20}
	673	2700	3.7×10^{-20}		753	120	3.6×10^{-19}
	698	1050	9.0×10^{-20}		763	60	7.6×10^{-19}

A distinct dependence of Q and D_0 on the size of the tracer atoms is observed for the ternary alloy, i.e., the values are higher for the larger tracers. The diffusion parameters are related according to

$$D_0 = A\exp\left(\frac{Q}{B}\right), \tag{2}$$

with constant fitting parameters A and B, as seen in the plot of $\ln D_0$ versus Q shown in Fig. 3. All data points (below and above T_g) can be fit with a single line, with factors $A=1.2\times10^{18}\ m^2\,s^{-1}$ and $B=0.067$ eV. It has been demonstrated that the diffusion behavior of various elements in metallic NiZr glasses is largely influenced by their atomic size and less by the differences of the chemical nature of the elements. Therefore, the following discussion is based on the size differences of the various tracer atoms.

The absolute values of the diffusion coefficients of different tracers are dependent on the atomic size of the tracer: smaller atoms are generally faster than larger ones, cf. Table I for a list of the atomic sizes. The diffusivity of Co, which can be regarded as a substitute for the smallest component of the alloy, Ni, is about two orders of magnitude greater than the diffusion coefficients of Ti. Ti is only slightly larger than the mid-sized component Al (cf. Table I). The difference in diffusion coefficients between Ti and Hf, the latter being of similar size as Zr, is only about one order of magnitude. It is

TABLE III. Activation enthalpies Q and pre-exponential factors D_0 in the temperature range below T_g.

Tracer	D_0 ($m^2\,s^{-1}$)	Q (eV)
Co	1.1×10^{-7}	1.63
Fe	2.8×10^{-7}	1.70
Cu	2.8×10^{-7}	1.70
Ti	8.5×10^{-5}	2.27
Hf	$3.7\times10^{+1}$	3.13

TABLE IV. Activation enthalpies Q and pre-exponential factors D_0 in the temperature range above T_g.

Tracer	D_0 ($m^2\,s^{-1}$)	Q (eV)
Co	$6.0\times10^{+0}$	2.66
Ti	$3.1\times10^{+5}$	3.56
Hf	$6.6\times10^{+13}$	4.83

remarkable, however, that the dependence of diffusion on size for the smaller atoms Co, Fe, and Cu, in comparison to that in the binary alloy Ni_xZr_{100-x}, is much less pronounced. Although their sizes are nearly the same, it should be recalled that the diffusion coefficient of Co in $Ni_{50}Zr_{50}$ at $T=573$ K is about 40 times larger than that of Cu.[1] This is also true for the amorphous alloy $Fe_{40}Ni_{40}B_{20}$ with the diffusion coefficient of Fe and Ni being nearly ten times the one of Cu.[17]

During the initial stage of the diffusion anneal, structural relaxation can lead to a reduction in the diffusion coefficients with time. This effect, however, is small in the present case, the diffusion coefficient decreases only by a factor of 2, as illustrated in Fig. 4. This is in agreement with the observation in $Ni_{19}Zr_{62}Al_{19}$ (Ref. 6); in Ni_xZr_{100-x}, not even this small relaxation effect was observed.[1]

B. Radiation-enhanced diffusion

The results for radiation-enhanced diffusion of Co in $Ni_{23}Zr_{62}Al_{15}$ are shown in Fig. 5. The observed diffusional broadening of the Co tracer consists of the temperature-independent ion beam mixing observed at the lowest irradiation temperatures and the temperature-dependent radiation-enhanced diffusion. Consequently, the diffusion coefficient is enhanced compared to the thermal diffusion, which is included for comparison in Fig. 5. In order to compare the results of the binary and ternary alloys, $Ni_{50}Zr_{50}$ and $Ni_{23}Zr_{62}Al_{15}$, data of the binary metallic glass were taken from Ref. 10; the diffusion coefficients, however, were normalized by the rate of damage energy deposition by plotting $Dt/\phi F_D$ vs $1/T$ as illustrated in Fig. 6. Here, ϕ is the ion fluence and F_D is the damage energy deposition per unit length normal to the specimen surface. For all tracers, $Dt/\phi F_D$ is nearly independent of temperature at lower temperatures and increases with temperature at higher temperatures. In both alloys, both small (Co, Cu) and large (Hf, Au) tracer atoms have been used. As seen in Fig. 6, RED depends more on the size of the tracer atoms than it does on the composition of the alloy. For the larger tracer atoms, the values of $Dt/\phi F_D$ are smaller and the onset of RED occurs at higher temperatures.

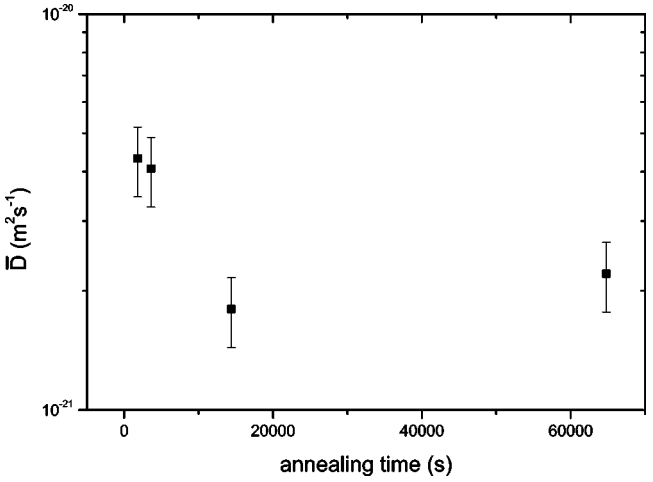

FIG. 4. Relaxation effect for the diffusion of Fe in $Ni_{23}Zr_{62}Al_{15}$ at $T=598$ K.

IV. DISCUSSION

If diffusion takes place via an interstitial mechanism, a pronounced dependence of the diffusion coefficient on the

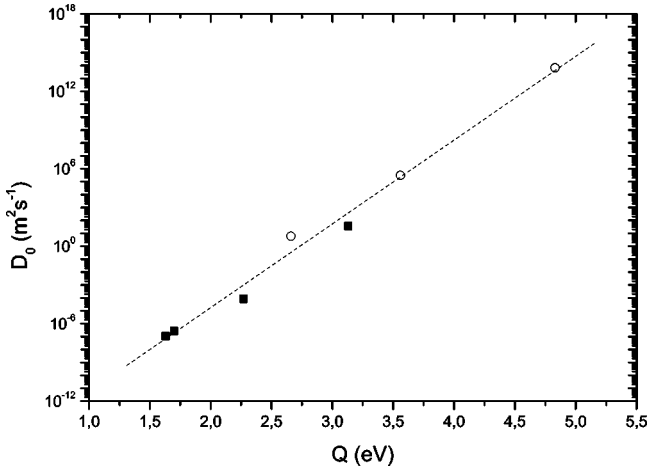

FIG. 3. Plot of the experimentally observed values of D_0 and Q for various tracers in $Ni_{23}Zr_{62}Al_{15}$. The filled symbols represent values in the glassy state, the open ones in the deeply supercooled state. The line is a linear fit to all the data points given.

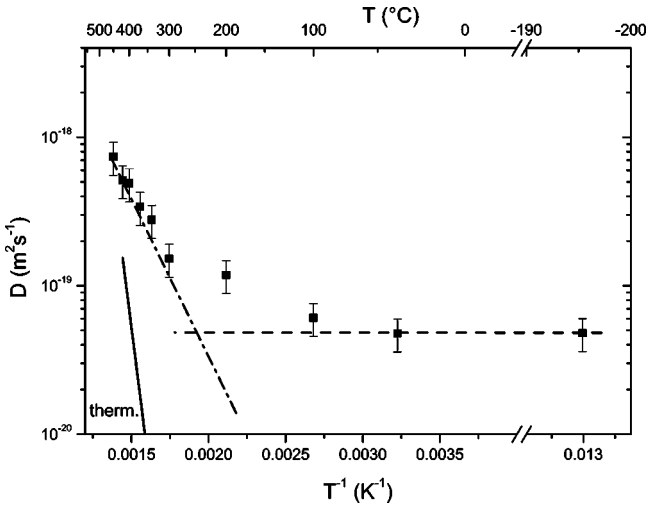

FIG. 5. Diffusivities of Co in $Ni_{23}Zr_{62}Al_{15}$ during irradiation with 1-MeV Kr^+ as a function of inverse temperature; the solid line represents the temperature dependence of the thermal diffusion, i.e., without irradiation.

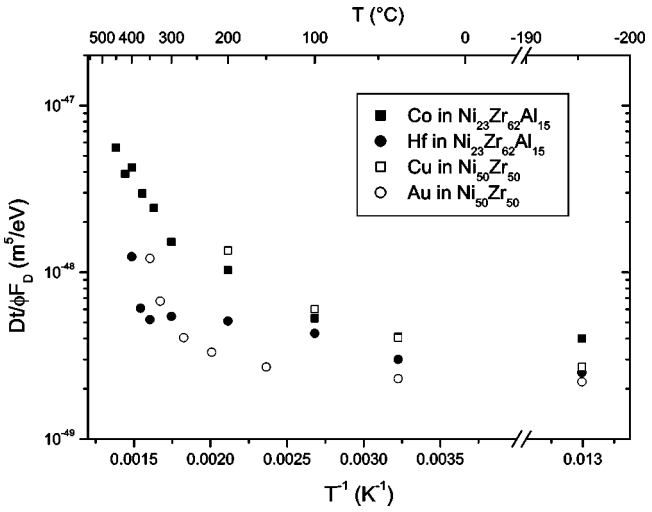

FIG. 6. Normalized diffusion coefficient, $Dt/\phi F_D$, as a function of inverse temperature.

atomic radius is expected, as observed in α-Zr and α-Ti.[18] The strong size dependence observed in *a*-NiZr thus led to the interpretation of the diffusion behavior of small tracer atoms in terms of an interstitial-like mechanism.[1] In contrast a collective diffusion mechanism, as assumed for larger atoms in metallic glasses, does not show such a pronounced size dependence of the diffusion coefficients. In $Ni_{23}Zr_{62}Al_{15}$, a distinct dependence on size is indeed observed for the tracers Co, Ti, and Hf, but there is almost no size dependence among the small atoms Co, Fe, and Cu, despite being very strong in α-Zr, α-Ti, and *a*-NiZr. A weak dependence on size was also observed for the diffusion of Ni, Co, and Fe in $Co_{58}Fe_5Ni_{10}Si_{11}B_{16}$ (Ref. 12) and in $Zr_{46.75}Ti_{8.25}Cu_{7.5}Ni_{10}Be_{27.5}$.[19,20] In comparison to the data and interpretations given in the literature, the diffusion behavior of tracer atoms with minor size differences can be explained assuming a collective diffusion mechanism even for the smallest transition metal tracers.

The isotope effect for a diffusion mechanism involving several surrounding atoms is expected to be small based on theoretical calculations. In metallic glasses, isotope effects ranging from $E=0$ to 0.1 have been found, indicating that ≈ 10 atoms are involved in the diffusion process.[21] Values of $E \approx 0.1$ have also been measured for several tracers in $Ni_{23}Zr_{62}Al_{15}$; these data will be published elsewhere.[22] It appears, therefore, that the addition of Al as a constituent to the binary metallic glass NiZr dramatically alters the diffusion of very small tracer atoms. Diffusion of Ni and Co takes place by individual atomic jumps in an interstitial-like mechanism in Ni_xZr_{100-x}, while Co diffuses by a collective process in a-$Ni_{23}Zr_{62}Al_{15}$. Reference 23 reported values of E close to zero even for the small tracer Co in Co_xZr_{1-x} with $0.31<x<0.86$, concluding a highly collective diffusion mechanism. Whether this is also valid for NiZr cannot be clarified without measurements; there exist, however, no measurements of the isotope effect in NiZr. In simulations of the diffusion in NiZr a high fraction of individual jumps of Ni was found.[24]

We also find that diffusion coefficients of small tracer atoms, such as Co, are dramatically reduced by the addition of Al to $Ni_{50}Zr_{50}$. For the larger tracer atoms, such as Hf, the diffusion coefficients in the binary and ternary metallic glasses are comparable below T_g. Above T_g the diffusion coefficients of Hf in the ternary alloy system become closer to those of small tracers, which is indicative of its higher value of the activation enthalpy. It must be pointed out that the value of D_0 for Hf according to Ref. 16 is rather low $(2.8\times10^{-9}\ m^2/s)$. This result contrasts with the observation that D_0 is usually higher with higher values of Q. It should be noted that the measurement of the diffusion of large tracers in amorphous metals is difficult due to the very small values of the diffusion coefficients.

It is noteworthy that the absolute values of the diffusion coefficients of the tracers in the ternary NiZrAl system at a given temperature are not necessarily the lowest in $Ni_{23}Zr_{62}Al_{15}$ alloy chosen for this study. It is observed, especially in the Al-richer/Ni-poorer region of this alloy system, that the diffusion is slower. Comparing the diffusion coefficients of the tracers Co and Ti in $Ni_{23}Zr_{62}Al_{15}$ with those in $Ni_{18}Zr_{57}Al_{25}$ and $Ni_{17}Zr_{64}Al_{19}$, which have been reported in Ref. 6, illustrates that the diffusion coefficients in the latter alloys are about one order of magnitude smaller at temperatures around 573 K. Comparing the diffusivities not at a fixed temperature but at a homologous temperature (i.e., normalized to the glass transition temperature T_g, that is given in Ref. 2), shows that $D(T_g)$ is, indeed, the lowest for $Ni_{23}Zr_{62}Al_{15}$. This conclusion is based on the data given here and in Ref. 6, and thus comprises only a few compositions. A more detailed description of the influence of the composition on the diffusivity will be published elsewhere.[22] The reduced atomic mobility in $Ni_{23}Zr_{62}Al_{15}$ relative to NiZr is also suggested by the small but measurable structural relaxation observed only in the ternary alloy. Due to the reduced atomic mobility, the as-prepared structure of the ternary amorphous alloy is not completely relaxed, as the atoms arriving at the surface do not have sufficient time to arrange compared to atoms in the binary alloys, at similar growth rates.

A distinct change of the slope in the Arrhenius plot is observed at temperatures above T_g, i.e., at ≈ 700 K. Even though the activation enthalpy Q and the pre-exponential factor D_0 increase above T_g, cf. Table IV, the correlation as given in Eq. (2) remains valid. Ref. 25 compared the values of Q and D_0 reported in the literature for some bulk metallic glasses in the glassy and deeply supercooled state and in conventional metallic glasses. These data were fit with a single line, the parameters being $A=4.8\times10^{-19} m^2\,s^{-1}$ and $B=0.056$ eV, which are close to those obtained here. The correlation of the values was interpreted by assuming a highly cooperative diffusion mechanism in both states, glassy and deeply supercooled liquid. This is consistent with the interpretation of the results of the diffusion experiments of different tracers given above.

The RED experiments demonstrate that irradiation induced defects can act as carriers for diffusion. When point defects are the carriers of the radiation-enhanced diffusion, the resulting enhancement is expected to be nearly the same for both alloys, $Ni_{23}Zr_{62}Al_{15}$ and $Ni_{50}Zr_{50}$. In the case of

thermal radiation, however, there are significant differences in the parameters describing the diffusion, i.e., Q and D_0, for larger tracers like Hf or Au: In $Ni_{50}Zr_{50}$, $D_0 \approx 1 \times 10^{-8}$ m^2/s and $Q \approx 1.8$ eV,[15,16] whereas the values are considerably higher in $Ni_{23}Zr_{62}Al_{15}$, cf. Table III. Thus point defects cannot contribute substantially to the thermal diffusion.

Lastly, it is illuminating to compare the present results of radiation-enhanced diffusion with reported values of radiation-induced viscous flow, which has been observed for a number of different amorphous materials, including $Cu_{27.5}Zr_{65}Al_{7.5}$, an alloy similar to the one investigated here.[26] In comparing these quantities, we first normalize the units of dose to the more physical units of displacements per atom and assume a displacement energy of 10 eV.[27] Then, assuming that viscous flow requires the diffusion of the least mobile component in the alloy, Zr, we obtain, $Dt/\phi F_D = 7.5 \times 10^{-19}$ m^2 dpa^{-1}. The radiation-induced viscosity can be expressed in terms of the fluidity, $H = t/\eta\phi F_D$, where η is the radiation-induced viscosity. If we next employ the Stokes-Einstein expression to relate diffusivity and viscosity, i.e.,

$$D = \frac{kT}{6\pi\eta R_o}, \tag{3}$$

we obtain $H \approx 3 \times 10^{-7}$ (Pa-dpa)$^{-1}$, which is ≈ 100 times the measured value. Here, we assumed a temperature of 600 K in Eq. (3). The discrepancy can be understood by recognizing from the magnitude of the radiation-enhanced diffusion coefficient that each created defect undergoes the equivalent of less than ≈ 10 nearest neighbor jumps. This means that diffusion is well localized around the sites where defects are created. Since the defects produced by heavy ion irradiation are highly concentrated in displacement cascades, the diffusion within the cascade is large, but outside the cascade it is negligible. After high dose irradiations, as is the case for these experiments, all regions are overlapped by cascades several times. This inhomogeneity in damage creation, therefore, has little effect on the diffusion measurements.

For radiation-induced viscous flow, however, the inhomogeneity of the damage cannot be ignored. Viscous flow occurs in the response to an applied stress. Once the stress is relaxed by the flow, all additional defect motion has no net effect. Thus, the large amount of defect motion in a cascade contributes linearly to the diffusion, but its contribution to flow saturates.

In summary, considering all thermal and RED data, the following comprehensive model for the diffusion in the binary NiZr and the ternary NiZrAl metallic glasses is proposed. In the binary $Ni_{50}Zr_{50}$ metallic glass small atoms such as Co can diffuse both by a collective and a single atomic jump process, with the interstitial-like process dominating by orders of magnitude. As a consequence of the interstitial-like mechanism, the diffusion coefficients of small tracers exhibit a large size dependence. The drastic decrease of the Co-diffusion coefficient in $Ni_{23}Zr_{62}Al_{15}$, compared to the binary metallic glass, is caused by a suppression of the interstitial-like mechanism by the increased packing of the amorphous matrix. Therefore, only the collective process contributes and thus controls the diffusion coefficients. As the collective mechanism does not have a significant size effect, the small differences of the atomic sizes between Co, Fe, and Cu do not result in observable differences of the diffusion coefficients. The diffusion of Hf in $Ni_{23}Zr_{62}Al_{15}$ is still reduced compared to the smaller atoms as the difference of the atomic size is greatly larger.

In the RED studies of the $Ni_{50}Zr_{50}$ system the enhancement of the diffusion was interpreted by the additional defect formation due to the ion irradiation and the reduced activation enthalpy.[10] As the thermal diffusion is considered to occur by an interstitial-like mechanism, i.e., a single jump process involving only individual atoms, this interpretation is straightforward. In the ternary amorphous alloy, $Ni_{23}Zr_{62}Al_{15}$, the results of the thermal diffusion give evidence for a collective mechanism for all atomic sizes. Therefore, the RED of small tracer atoms in the $Ni_{23}Zr_{62}Al_{15}$ is not expected to be as well defined as in the binary metallic glass. However, it can be concluded that in addition to the collective motion of the small atoms, ion irradiation creates a sufficiently large number of single defects and thus, small atoms have an additional avenue for diffusion. Finally, the Stokes-Einstein relation is not obeyed in irradiated amorphous alloys, presumably owing to the inhomogeneous nature of the damage process.

V. CONCLUSIONS

The reduction of the diffusivity in $Ni_{23}Zr_{62}Al_{15}$ compared to NiZr, as proposed in Ref. 2, is confirmed. The investigated dependence of the tracer diffusion on atomic size with no significant differences for the three smaller tracer atoms Co, Fe, and Cu is interpreted with the suppression of defect type diffusion paths available in the binary amorphous alloys. This limits the diffusion path also for the small atoms to a collective diffusion mechanism. Radiation-enhanced diffusion was observed, with the same normalized diffusion coefficients as in $Ni_{50}Zr_{50}$.

ACKNOWLEDGMENTS

The authors would like to thank R. Nagel for the RBS measurements, A. Berendes for the higher temperature annealings. This work was supported by the DFG Schwerpunkt-Programm *"Unterkühlte Metallschmelzen: Phasenselektion und Glasbildung"* and in part by the Department of Energy, Basic Energy Sciences under Grant No. DEFG02-91-ER45439.

[1] H. Hahn and R. S. Averback, Phys. Rev. B **37**, 6533 (1988).
[2] A. Inoue, T. Zhang, and T. Matsumoto, Mater. Trans., JIM **31**, 177 (1990).
[3] K. Knorr, M.-P. Macht, and H. Mehrer, in *Bulk Metallic Glasses*, edited by William L. Johnson, Akihisa Inoue, and C. T. Liu, MRS Symposia Proceedings No. 554 (Materials Research Society, Pittsburgh, 1999), p. 269.
[4] Z. Altounian, T. Guo-Hua, and J. O. Strom-Olsen, J. Appl. Phys. **54**, 3111 (1983).
[5] L. Q. Xing and P. Ochin, Acta Mater. **45**, 3765 (1997).
[6] S. Flege, U. Fecher, and H. Hahn, J. Non-Cryst. Solids **270**, 123 (2000).
[7] Y. Qiu, U. Geyer, S. Schneider, M.-P. Macht, W. L. Johnson, and T. A. Tombrello, Nucl. Instrum. Methods Phys. Res. B **117**, 151 (1996).
[8] U. Geyer, W. L. Johnson, S. Schneider, Y. Qiu, T. A. Tombrello, and M.-P. Macht, Appl. Phys. Lett. **69**, 2492 (1996).
[9] V. Zöllmer, K. Rätzke, F. Faupel, A. Rehmet, and U. Geyer, Phys. Rev. B **65**, 220201 (2002).
[10] R. S. Averback and H. Hahn, Phys. Rev. B **37**, 10383 (1988).
[11] A. K. Tyagi, M.-P. Macht, and V. Naundorf, J. Nucl. Mater. **179-181**, 1026 (1991).
[12] P. Scharwaechter, W. Frank, and H. Kronmüller, Z. Metallkd. **87**, 885 (1996).
[13] T. Schuler, P. Scharwaechter, and W. F. J. Frank, in *Microstructural Processes in Irradiated Materials*, edited by S. J. Zinkle, G. Lucas, R. Ewing, and J. Williams, MRS Symposia Proceedings No. 540 (Materials Research Society, Pittsburgh, 1999), p. 195.
[14] F. Faupel, W. Frank, M.-P. Macht, H. Mehrer, V. Naundorf, K. Rätzke, H. R. Schober, S. K. Sharma, and H. Teichler, Rev. Mod. Phys. **75**, 237 (2003).
[15] R. S. Averback, MRS Bull. **16**, 47 (1991).
[16] Y. Loirat, J. L. Bocquet, and Y. Limoge, Mater. Sci. Forum **269-272**, 649 (1998).
[17] S. K. Sharma, M.-P. Macht, and V. Naundorf, Acta Metall. Mater. **40**, 2439 (1992).
[18] H. Nakajima, M. Koiwa, Y. Minonishi, and S. Ono, Trans. Jpn. Inst. Met. **24**, 655 (1983).
[19] P. Fielitz, M.-P. Macht, V. Naundorf, and G. Frohberg, J. Non-Cryst. Solids **250-252**, 674 (1999).
[20] K. Knorr, M.-P. Macht, K. Freitag, and H. Mehrer, J. Non-Cryst. Solids **250-252**, 669 (1999).
[21] H. Ehmler, K. Rätzke, and F. Faupel, J. Non-Cryst. Solids **250-252**, 684 (1999).
[22] S. Flege and H. Hahn, (unpublished).
[23] A. Heesemann, V. Zöllmer, K. Rätzke, and F. Faupel, Phys. Rev. Lett. **84**, 1467 (2000).
[24] H. Teichler, Defect Diffus. Forum **143**, 717 (1997).
[25] S. K. Sharma and F. Faupel, J. Mater. Res. **14**, 3200 (1999).
[26] S. G. Mayr and R. S. Averback, Phys. Rev. Lett. **87**, 196106 (2001).
[27] S. G. Mayr, Y. Ashkenazy, K. Albe, and R. S. Averback, Phys. Rev. Lett. **90**, 055505 (2003).